Femtosecond Radiation Experiment Detector for X-Ray Free-Electron Laser (XFEL) Coherent X-Ray Imaging

Hugh T. Philipp, Lucas J. Koerner, Marianne S. Hromalik, Mark W. Tate, and Sol M. Gruner

Abstract—A pixel array detector (PAD) module has been developed at Cornell University for the collection of diffuse diffraction data in anticipation of coherent X-ray imaging experiments that will be conducted at the Linac Coherent Light Source (LCLS) at the SLAC National Accelerator Laboratory. The detector is designed to collect X-rays scattered from monochromatic femtosecond pulses produced by the LCLS X-ray laser at framing rates up to 120 Hz. Because X-rays will arrive on femtosecond time scales, the detector must be able to deal with instantaneous count-rates in excess of 10^{17} photons per second per pixel. A low-noise integrating front-end allows the detector to simultaneously distinguish single photon events in low-flux regions of the diffraction pattern, while recording up to several thousand X-rays per pixel in more intense regions. The detector features a per-pixel programmable two-level gain control that can be used to create an arbitrary 2-D, two-level gain pattern across the detector; massively parallel 14-bit in-pixel digitization; and frame rates in excess of 120 Hz. The first full-scale detector will be 1516×1516 pixels with a pixel size of 110×110 microns made by tiling CMOS ASICs (Application Specific Integrated Circuits) that are bump-bonded to high-resistivity silicon diodes. X-ray testing data of the first 185×194 pixel bump-bonded ASICs is presented. These are tiled to make the final detector. The measurements presented include confirmation of single photon sensitivity, pixel response profiles indicating a nearly single-pixel point spread function, radiation damage measurements and noise performance.

Index Terms— Free electron lasers, radiation detectors, semiconductor device measurement, silicon radiation detectors, X-ray detector, X-ray detectors, X-ray lasers.

I. INTRODUCTION

NEW high-intensity X-ray sources like X-ray Free-Electron Lasers (XFEL) are opening new possibilities into the types of X-ray studies that can be performed. It is anticipated that coherent, intense, femtosecond time-scale pulses produced by XFELs will allow the study of single, noncrystalline particles (such as large proteins, protein complexes or nano-particles) to be studied by collecting diffraction data from their electron density distributions [1]–[3]. Even though the energy absorbed by a particle during an ultra-intense XFEL pulse will destroy its chemical structure because of massive ionization and a subsequent Coulomb explosion of the sample, a pulse that is short enough should still yield relevant scattering information directly related to the original electron density of the particle. This is because the Coulomb explosion of the particle is rate limited by the acceleration of ionized particles/atoms. If the pulse is short enough, the X-rays are scattered before the Coulomb explosion occurs [1].

The experimental setup, collection of data, and analysis of the collected data are nontrivial. Even if the X-ray pulse is short enough in duration and intense enough to produce the desired scattering pattern, other technological issues are noteworthy and critical to the success of the experiment, including arranging temporal and spatial overlap of very short pulses and single particles, the orientation of the particles in the X-ray beam, and the best X-ray data collection strategy. Complicating matters, many frames of valid scattering data from identical particles are needed for reconstruction because much of the scattering pattern, particularly in important high-q (large scattering angle) regions, will be extremely low flux. For the experiment being considered, the expected flux in these regions is less than one photon per pixel. Another difficulty is that in most single particle scattering schemes, the orientation of the particle is not determined and the scattering patterns must be classified after the fact based on similarities of the Poisson noise-limited scattering patterns themselves.

The pixel array detector presented here is an answer to the technological question of how to collect the scattering patterns for the coherent X-ray imaging (CXI) of single particles at the Linac Coherent Light Source (LCLS) XFEL. Many of the detector characteristics are tailored specifically for the demands of the experiment, some of which are mentioned above. Specific technical requirements include the ability to distinguish whether or not single X-ray photons have been detected in any given pixel, while maintaining the ability to detect thousands ($>$ 2500) of X-rays per pixel in other parts of the scattering pattern. This is particularly notable since for a pulse that approaches 10 fs in length, the instantaneous count rate for some pixels will be greater than 10^{17} photons per second. This count rate alone excludes the possibility of using a photon counting detector. Another notable technical requirement, related to the ability to dis-

tinguish single photons, is a pixel-limited point spread function. In addition, the detector must be able to sustain a continuous frame-rate of 120 Hz. This follows from the operating procedures planned for the LCLS, and the high number of frames required for reconstructing the electron density from the diffuse X-ray scattering patterns produced by coherent X-ray imaging of noncrystalline samples.

II. PHYSICAL CONSTRUCTION OF PIXEL ARRAY DETECTOR (PAD)

A PAD is composed of two layers, the detector layer and the signal processing layer. These layers are mated together with isolated, pixel-level connections using solder bump-bonding (Bump bonding done by RTI, International Center for Materials and Electronic Technologies, Research Triangle Park, NC, USA). The detector layer is an array of diodes (Detector diode manufactured by SINTEF, NO-7465 Trondheim, Norway) made from 500 μm thick high-resistivity ($5 - 10$ kΩ) n-type silicon. The thickness of the diode layer gives a high quantum efficiency, greater than 0.99, when detecting 8 keV X-rays. The high resistivity of the diodes ensures over-depletion when a bias voltage of 200 V is applied. In operation, incident X-rays are absorbed by the silicon in the diodes and converted into charge carrier pairs. These charges migrate according to the applied electric field and the respective mobilities of the charge carriers. For the PAD presented, holes are collected (reasons for this are explained elsewhere [4]) by the signal processing layer through pixel-level connections. The signal processing layer is a 0.25 μm CMOS, mixed-mode application specific integrated circuit (ASIC) manufactured by TSMC (Taiwan Semiconductor Manufacturing Company Limited, No. 25, Li-Hsin Road, Hsinchu Science Park, Hsin-Chu 300, Taiwan). Each pixel of the ASIC has dedicated circuitry for processing the charge collected from the diode. The pitch of the pixel connections across the 2-D detector array is 110 μm. The size of the single pixel layout in the CMOS ASIC corresponds to the pitch (i.e., the pixel size is 110 μm $\times$ 110 μm).

III. PIXEL-LEVEL DESIGN AND OPERATION

A. Pixel Operation Description

A high-level schematic of the pixel is shown in Fig. 1. X-ray induced charge in the diode is collected at the 'in' node and integrated onto the feedback capacitance of the front-end capacitive transimpedance amplifier. The total feedback capacitance can be set to either the capacitance of cap1 or the sum of cap1 and cap2 to configure the gain (volts per integrated unit of charge) of the front-end. The selection of the capacitance is determined by 1-bit in-pixel memory that can be individually programmed for each pixel in the array. The capacitance of the feedback loop with and without cap2 as part of the integrating feedback loop is 565 fF and 75 fF, respectively. Since X-ray conversion in silicon produces 1 electron-hole pair per 3.65 eV of absorbed energy, the gain of the front-end stage is either 0.62 mV per 8-keV X-ray (low gain) or 4.7 mV per 8-keV X-ray (high gain). Since the usable voltage range of a pixel's analog stage is conservatively set to 1.7 V (set by the ramp, the digitization clock and Vref), the
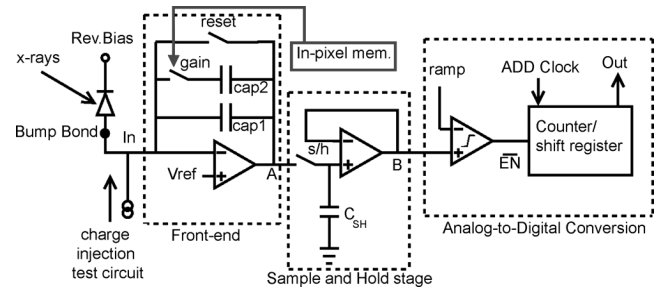

Fig. 1. High-level schematic of the pixel showing the major functional components: The front-end amplifier, the sample-and-hold buffer, and the digitization components. An in-pixel programmable gain mechanism is also shown. Figure reproduced with permission from [5] (2009, IOP Publishing Ltd.).

saturation of the pixel during normal operation is approximately 2700 X-rays in low-gain and 360 X-rays in high-gain.

After the charge is integrated by the front-end, the voltage at node A is sampled by the sample-and-hold stage and held constant during the next stage of in-pixel data acquisition, which is digitization.

During digitization, the voltage at node B is compared to a globally transmitted ramp, while a global analog-to-digital conversion (ADC) clock increments an in-pixel 14–bit counter. When the voltage of the ramp crosses the voltage held at node B, the counter is disabled and the value of the counter is taken to be proportional to the total charge integrated by the pixel. The digitized value of each pixel is then shifted onto a digital bus with a readout clock. These values are the output of the PAD. The digitization method is similar to that presented in [6].

B. Waveforms and Pixel Timing

Fig. 2 shows a simplified timing diagram for the pixel operating in a mode compatible with the requirements of the LCLS CXI experiment, including a frame rate of 120 Hz to match the repetition rate of the LCLS XFEL. The integration time shown is a small fraction of the framing period and in normal operation only spans 10 μs. The integration time is, however, much longer than the X-ray pulse produced by the XFEL and there are several reasons for this. The most important reason is that the leakage currents measured in diodes show that the integrated charge from the diode is expected to be much less than the charge from one 8-keV X-ray and measurements on the detector have demonstrated no discernible performance benefit by going to shorter integration times. Imposing a shorter integration time would only arbitrarly increase timing constraints in the experimental setup with no discernable performance improvement. After the integration time, the output voltage is sampled and digitized. Digitization in normal operation takes 4 ms, occurring simultaneously for all pixels. Pixel read out then proceeds and requires addressing (not shown in Fig. 2). Each pixel is addressed and readout by switching the counter to act as a shift-register. Readout of the ASIC takes approximately 3.2 ms.

IV. CHIP-LEVEL ARCHITECTURE

The 2-D detector array comprises eight banks of identical pixels with every column being a mirror image of its nearest neighbor columns for efficient sharing of digital and analog
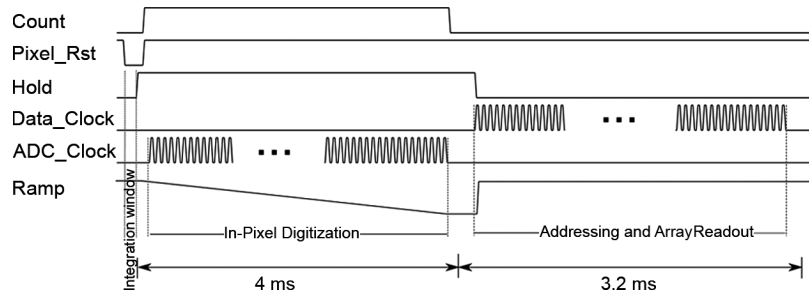
Fig. 2. A simplified timing diagram of the detector showing a division between exposure time, digitization, and detector readout. The planned exposure time for the CXI experiment is $10 \ \mu$s.

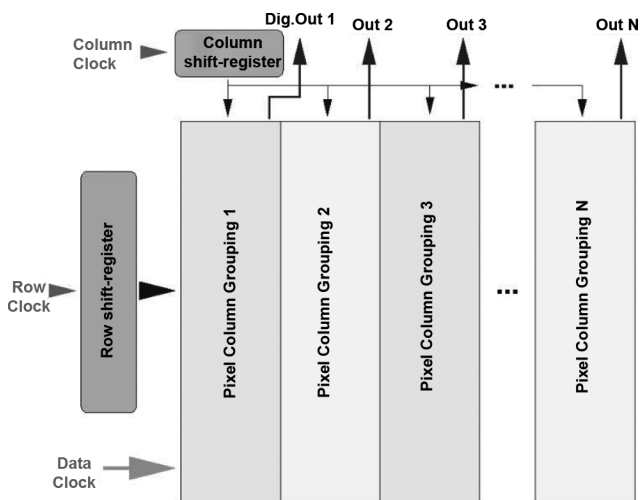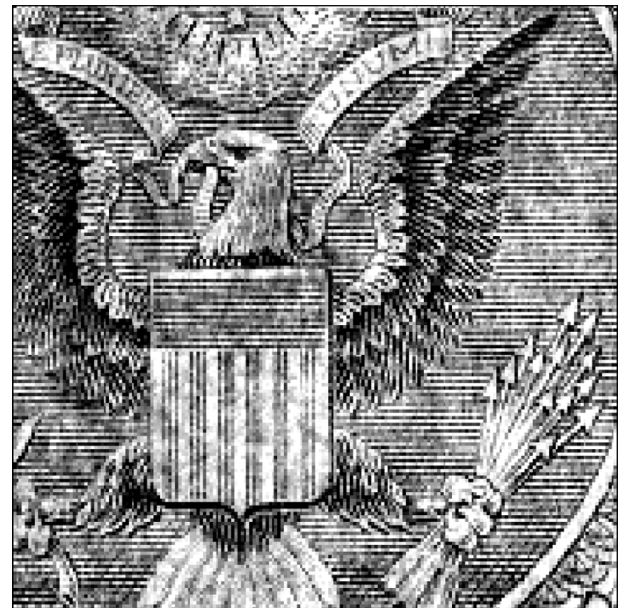Fig. 3. Chip level architecture: The pixels are grouped in eight banks ($N = 8$).

Fig. 4. An X-ray radiograph of a U.S. one dollar bill. The X-ray source used was a copper anode X-ray tube. The features of the one dollar bill are about the same size as the pixel pitch. Figure reproduced with permission from [5] (2009, IOP Publishing Ltd.).

buses on the ASIC. The general structure is shown in Fig. 3. Seven of these banks are 26×185 pixels and one bank is 12×185 pixels. The total dimensions of the array itself, approximately $21 \ \text{mm} \times 21 \ \text{mm}$, are constrained by limits of the die size offered by the commercial CMOS process used. The banks are addressed using two shift registers that pass a bit to activate the column or row desired. The column shift-register, which has 26 output positions, is fanned out to the eight banks so that corresponding columns in each bank are addressed in parallel. Each bank has a dedicated digital output. Full readout of the array is accomplished in 3.2 ms using a 25 MHz data clock. The output from the array is completely digital. The data acquisition process is controlled with an FPGA interface board based on the Xilinx XC4V100FX FPGA. This board provides an interface to a PCI-Express bus [7].

V. Testing Results

Bump-bonded modules have been tested and verified to be fully functional and appropriate for the experiment. Full-speed readout and real-time framing has been verified for sustained continuous acquisition of data. Fig. 4 is a radiograph of part of a United States one dollar bill, verifying correct ordering of the data. Measurements of the single pixel saturation values for nominal operating conditions are in accordance with the anticipated values, namely, ≈ 360 8 keV X-rays for high-gain and ≈ 2700 8 keV X-rays for low-gain. The anticipated values were

designed using the feedback capacitances of the integration stages and the available voltage swing of the front-end amplifier. Measurements assumed that saturation was reached when the input signal to ADC curve obtained flattened and deviated from linearity by 2%. The signal-to-noise ratio for detecting a single 8-keV photon was measured to be approximately 7 for high-gain mode and approximately 2 for low-gain mode.

A. Single Photon Sensitivity

The PAD in the CXI experiment must faithfully record the number of photons incident on the detector in low flux regions. This requires a signal-to-noise ratio large enough to clearly distinguish quanta associated with single photon events. Fig. 5(a) shows a histogram of the output of a single pixel in high-gain mode over more than 4000 frames with a $75 \ \mu$m diameter pinhole masking most of the charge sharing regions on the pixel perimeter. The X-ray source used was an X-ray tube with a copper anode run at 14 kV, 0.7 mA. A $50 \ \mu$m thick nickel filter suppressed the bremsstrahlung spectrum and Cu K$_\beta$ radiation. The resulting beam was nearly monochromatic with an energy
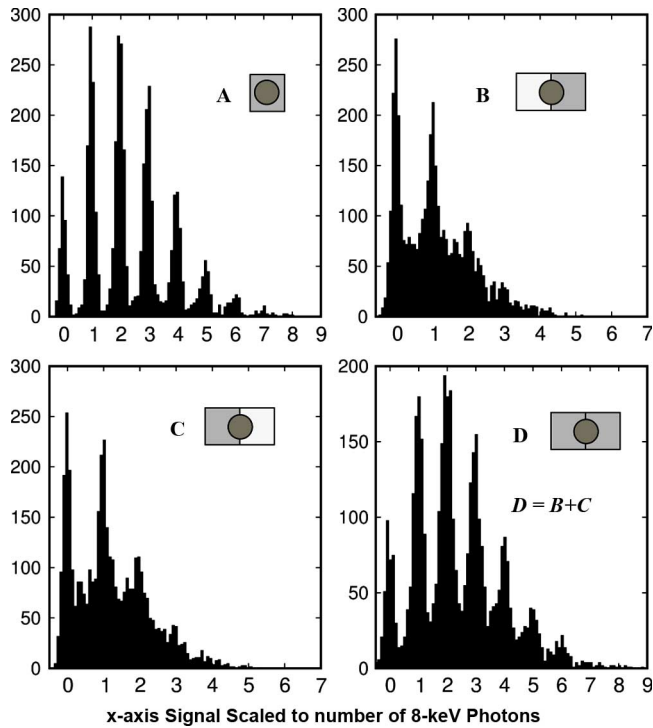
Fig. 5. Histograms of pixel outputs over thousands of frames. Sub-figure (a) is from a pixel illuminated through a 75 micron pinhole. The pinhole reduces charge being shared with other pixels. Sub-figures (b) and (c) show similar histograms of two adjacent pixels with the pinhole positioned on the border between the pixels. Sub-figure (d) shows a histogram of the per-frame sum of the two pixels (b and c) for the same data set.

TABLE I
DETECTOR SPECIFICATION SUMMARY

Pixel Size	$110\,\mu m \times 110\,\mu m$	
Array Size	Single ASIC:	185×194
	Tiled Detector :	1516×1516
Frame Rate	120 Hz in operation at LCLS	
Pixel Saturation	2700	8-keV x-rays (Low-Gain)
	350	8-keV x-rays (High-Gain)
Quantum Efficiency	0.97	8-keV x-rays
	0.89	12-keV x-rays
	0.48	18-keV x-rays
Signal-to-Noise Ratio	7 for 8-keV x-ray (High-Gain)	
(rms)	2 for 8-keV x-ray (Low-Gain)	

a factor of $\sqrt{2}$) than the noise associated with a single pixel. Peak values less in Fig. 5(d) than Fig. 5(a) because addition is per frame, the results of which are histogrammed. Additional noise caused by summing of independent pixels results in fewer events per histogram bin.

B. Line Spread Function

Directly collecting charge produced by X-rays absorbed in a fully-depleted silicon detector layer has several advantages over X-ray detector methods that rely on detecting secondary optical photons emitted by a phosphor. One of these advantages is a comparatively superb point spread function. This is because after the charge is produced, it is directly collected by the applied electric field. The spread of charge during the time it takes to migrate through the detector layer to the pixel connection may give rise to charge sharing between pixels. Measurement of charge sharing and pixel response as a function of position of incident photons can be accomplished by measuring the line spread function with a knife-edge that is held at a slight angle to the column (or row) so that varying degrees of pixel exposure are collected as a function of position along a knife edge illuminated with a flat field. Additional, finer resolution data can be gathered by translating the detector behind the X-ray illuminated knife edge. A measurement of this sort is shown in Fig. 6. Pixel output is plotted as a function of mean knife edge position with respect to the pixel center. The derivative of this, also shown, gives the line spread function. The line spread function recovered is the convolution of the charge spreading in one dimension with a one-dimensional box function having the same width as the pixel ($110\,\mu m$). The results of the measurements show discernible charge sharing up to $20\,\mu m$ from the nominal pixel boundary. Beyond this charge sharing region, the line spread function is flat and dominated by pixelization. Since the pixels are $110\,\mu m$ wide, the line spread and point spread functions are pixel-size limited. The width of the charge sharing region does, however, indicate that a significant percentage (up to 60%) of randomly distributed incident photons will be affected by charge sharing to some degree, as they will be within $20\,\mu m$ of the pixel boundary.

C. Radiation Testing

Radiation damage of the bump-bonded pixel array detector was tested up to 750 kGy (Si) referenced to the face of the detector using an 8-keV X-ray source. The results indicate that

corresponding to the Cu K_α line (8.04 keV). The result is a histogram with clearly distinguishable peaks corresponding to an integer number of photons detected. The peaks correspond to 0, 1, 2, …, etc., 8 keV photons. Using this data the approximate signal-to-noise-ratio for a single 8-keV photon is approximately 7 (signal detected from a single absorbed photon over one standard deviation noise derived from repeated measurements). Another result is that the signal for a single photon incident upon a pixel, in a region with no charge sharing, can yield information on the photon energy. The detector is, however, not intended to be used for energy discrimination but to record the signal produced by integer numbers of monochromatic, elastically scattered photons from an XFEL experiment. Performance characteristics are shown in Table I.

When an X-ray illuminated pinhole is positioned so that its projection straddles the border between two pixels, a significant number of the photons incident on the detector convert in charge sharing regions where the charge produced by an absorbed photon is split between pixels. Since only a fraction of the charge produced by a charge sharing event is collected by an individual pixel, histograms of single pixel outputs over many frames do not show a clear quantized response. This effect is shown in Fig. 5(b) and (c). In this case, the total charge deposited by a given X-ray event remains constant and a histogram of the frame-by-frame sum of the two pixels (calculated after a small gain correction) recovers discernible X-ray peaks (5D). There is, however, a degradation in the quality of the histogram because the noise associated with the sum of pixels is greater (by
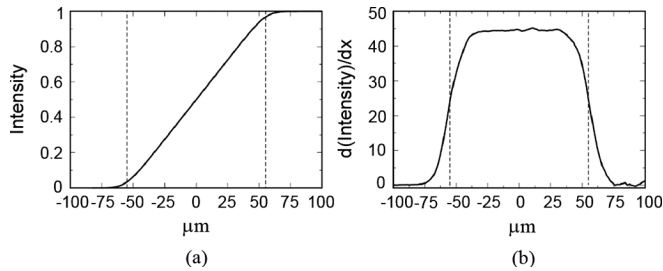
Fig. 6. (a) Knife edge response and (b) line response of a 50 μm thick tungsten knife edge.

leakage currents of the diode increase, but the impact on data collected for the proposed experimental application will be minimal. As reported in [5], upon dosing the leakage current increased from 44 fA per pixel to 124 fA per pixel. This indicates the noise component from diode leakage current will increase by a factor of approximately 2/3, but the noise associated with this is still only approximately three electrons, whereas the total noise in equivalent signal electrons (or holes) is two orders of magnitude greater. Dose testing of the unbumped ASIC indicates that damage to the CMOS is recoverable by annealing. The annealing was done primarily at room temperature over a couple months. More information on radiation testing of the detector can be found in [5].

VI. CONCLUSION

The division of labor on this detector project is that Cornell is charged with developing and testing a single-ASIC module and SLAC is charged with assembling and calibrating the modules into a full size tiled detector. As described herein, the module has been successfully developed and meets the required specifications. Modules consisting of two ASICs per double-wide diode layer are presently being assembled by the SLAC team into the full sized detector array.

The ability to distinguish single photon events and also integrate thousands of photons at extremely high count rates may be a hallmark of X-ray free electron laser experiments. New X-ray sources with extremely high peak brilliances require detectors that allow scientists to realize their full scientific potential. This detector represents one of the first detectors specifically designed for these new sources that has been completed to the stage of large-scale tiling and imminent installation on an X-ray Free Electron Laser beamline for coherent X-ray imaging. SLAC has already installed a tiled version of this detector in the X-ray pump probe (XPP) beamline at the LCLS.

This detector is, beyond an answer to the requirements of one experiment, a template for further detector development. In-pixel digitization, for instance, is an increasing trend in CMOS imaging detectors for X-ray science. A purely digital pixel output has the advantage of simplified readout electronics and avoids pitfalls of high-speed analog multiplexing and

eases some aspects of large-scale tiling. Adjustable front-end gain is another feature likely to be used more often in charge integrating detector designs because it effectively increases the dynamic range of the detector. There are other methods for increasing the dynamic range [8], [9], but these often limit instantaneous count rates to levels that are incompatible with new, brighter X-ray light sources being developed. The measurements of charge sharing demonstrates an important advantage of charge integrating detectors that is often lost with counting detectors. This advantage is complete measurement of deposited charge independent of the location of X-ray conversion with respect to pixel borders.

When using a detector in the realm where loss of charge through recombination is small, the measurement of charge collected by an integrating front-end is a direct measurement of the X-ray energy absorbed in the detector. In contrast, detectors that count photons based on pulse shape analysis using discrimination levels are hindered by count-rate limitations and charge sharing between pixels. At very high count-rates like those anticipated in many XFEL experiments, photon counting is not possible.

REFERENCES

[1] R. Neutze, R. Wouts, D. van der Spoel, E. Weckert, and J. Hajdu, "Potential for biomolecular imaging with femtosecond X-ray pulses," *Nature*, vol. 406, no. 6797, pp. 752–757, Aug. 2000.

[2] N.-T. D. Loh and V. Elser, "Reconstruction algorithm for single-particle diffraction imaging experiments," *Phys. Rev. E (Statistical, Nonlinear, and Soft Matter Physics)*, vol. 80, no. 2, p. 026705, 2009.

[3] G. S. A. H. J. Huldt, "Diffraction imaging of single particles and biomolecules," *J. Structural Biology*, vol. 144, pp. 219–227, 2003.

[4] S. L. Barna, "Development of a microsecond framing two-dimensional pixel array detector for time-resolved x-ray diffraction," Ph.D. dissertation, Cornell University, Ithaca, NY, 1997.

[5] L. J. Koerner, H. T. Philipp, M. S. Hromalik, M. W. Tate, and S. M. Gruner, "X-ray tests of a pixel array detector for coherent X-ray imaging at the linac coherent light source," *J. Instrumentation*, vol. 4, no. 03, p. P03001, 2009.

[6] S. Kleinfelder, S. Lim, X. Liu, and A. E. Gamal, "A 10 000 frames/s CMOS digital pixel sensor," *IEEE J. Solid State Circuits*, vol. 36, no. 12, pp. 2049–2059, 2001.

[7] M. S. Hromalik, H. T. Philipp, L. J. Koerner, M. W. Tate, and S. M. Gruner, "Data acquisition and control for a pixel array detector (PAD) for single particle scattering at the linac coherent light source (LCLS)," in *Proc. 2007 IEEE Nucl. Sci. Symp. Conf. Record*, 2007, pp. 1744–1750.

[8] D. Schuette, "A mixed analog and digital pixel array detector for sychrotron x-ray imaging," Ph.D. dissertation, Cornell University, Ithaca, NY, 2008.

[9] W. Vernon, M. Allin, R. Hamlin, T. Hontz, D. Nguyen, F. Augustine, S. M. Gruner, N. H. Xuong, D. R. Schuette, M. W. Tate, and L. J. Koerner, "First results from the 128 × 128 pixel mixed-mode Si X-ray detector chip," *Hard X-Ray and Gamma-Ray Detector Physics IX*, vol. 6706, no. 1, p. 67060U, 2007.